Diaphragm Design Improvement for a Metering Pump

Giovanni Mimmi[*]
Dipartimento di Meccanica Strutturale
Università degli studi di Pavia
Via Ferrata, 1
I-27100 Pavia, Italy
phone: +39-0382-505.452
fax: +39-0382-528.422
e-mail: mimmi@unipv.it

Paolo Pennacchi
Dipartimento di Meccanica
Politecnico di Milano
P.zza L. da Vinci, 32
I-20133 Milano, Italy
phone: +39-02-2399.4783
fax: +39-02-7063.8377
e-mail: paolo.pennacchi@mecc.polimi.it

ABSTRACT

Since the membrane has to separate the process fluid from the oil circuit in metering diaphragm pumps, it is the critical component of these machines. Sometimes, depending on the operating conditions, the membrane may crack and it is necessary to disassemble the pump and replace this component part. Therefore it is important to improve the design of the membrane to avoid this.

In this paper, the behaviour of a membrane mounted in a metering diaphragm pump has been simulated by using f.e.m. An accurate analysis of the results has allowed the membrane to be redesigned in a more rational way and to improve its performance.

Keywords: plunger-diaphragm metering pumps, design improvement, crack, composite materials

INTRODUCTION

Reciprocating metering pumps have two basic construction schemes: metering plunger pump and metering plunger-diaphragm pump. Both models are capable of producing to produce a very wide range of flow rate (from 10^{-3} to 1 m^3/h), since the plunger is driven by a variable stroke crank mechanism. Basic schemes of the two types of pumps are shown in figure 1.

Since these pumps are mainly employed in chemical, petrochemical and foodstuffs industries, process fluids are sometimes corrosive and often expensive, it is necessary for the pumps to have an almost perfect seal to avoid fluid leakage and to prevent process and working fluid from mixing.

In the metering plunger pump (left in figure 1) there is only one seal zone made of rings that separates working fluid from process fluid Due to the relative motion of plunger and cylinder, the wear may reduce the seal.

[*] Corresponding author

On the other hand, in the metering plunger-diaphragm pump, the plunger moves the process fluid through the elastic deformation of the diaphragm, so the relative motion in the sealing zone becomes less important[1].

The three main feature, which the diaphragms for metering pumps must possess, are:

- chemical inertia in the presence of process and working fluids;
- elastic behaviour;
- great resistance under cyclical stresses.

The chemical inertia requirement is usually satisfied by employing materials like PTFE (*Teflon*). If the temperature of the process fluid is too high for the PTFE, the diaphragm is made of a thin steel disk with a finished surface.

However, as a consequence of its high Young's modulus, the PTFE limits the elasticity of the diaphragm. For this reason it is necessary to use composite diaphragms: the side towards working circuit is made of NBR rubber while the other side is coated by a *Teflon* layer.

Usually the design of the rubber-*Teflon* diaphragm has been based on practical experience. The small amount of information about the material strength and the composite nature of the diaphragm make it difficult to estimate its actual behaviour and strength under working conditions.

The market demand for more performing metering diaphragm pumps - which are able to operate at higher temperature and pressure - confirms that the diaphragm is the critical component of the pump and also confirms the necessity for simulation tools to design this component.

Laboratory tests and real operating condition experiences have shown that the cracks are localised on the *Teflon* coating.

These cracks increase in size when the working pressure rises and interfere with the functionality of the pump because they deprive the diaphragm of its chemical inertia.

Once we had verified that the diaphragm assembling operation had not caused the damage, we decided to simulate the behaviour of the diaphragm under different working conditions by means of a f.e.m. to understand the causes of the cracks.

The aim of the simulations is to help designers by finding a relation between the shape of the diaphragm and its behaviour.

[1]See the classification proposed in [1] for the evaluation of the seal in plunger and diaphragm pumps.

PUMP OPERATION

We have analysed a reciprocating metering diaphragm pump with double ball valves. A basic scheme of the pump is shown in figure 2.

The plunger ①, moving in the direction shown in figure 2, moves the oil contained in the chamber ② and causes the movement and the deformation of the diaphragm ③. This causes the reduction of the volume occupied by the process fluid in the pumping head. The pressure rises in chamber ④ so that the valve ⑥ can open. Therefore, when the plunger moves in the opposite direction, the diaphragm deformation increases the volume ④. Furthermore a little reduction in pressure is produced in the pumping head and this causes the valve ⑥ to close and the inlet valve ⑤ to open.

The amount of fluid pumped at each cycle is obviously a function of the volume variation induced in the chamber ④ by the diaphragm deformation. This depends on the variation in volume of chamber ② that is a function of the diameter and the plunger ① stroke.

The diaphragm ③ is composite and axial-symmetric (see figure 3). The side facing the working circuit is made of rubber while the side facing the process fluid is coated with a uniform *Teflon* layer which has a protective function.

The simulations have been based on the hypothesis that material deformations are in a range of linear elastic behaviour. If we consider that each material is homogeneous and isotropic, only two physical constants are needed to express all coefficients of Hooke's law: Young's modulus E and Poisson's coefficient ν.

We have assumed that $\nu = 0.5$, $E_{\text{rubber}} = 4.7$ MPa (see PTFE DIN 53457) and $E_{Teflon} = 700$ MPa (see DIN 53504).

As a consequence of the low accelerations and the small displacements of the diaphragm during the pumping action - about 2-4 mm for membranes with a diameter of 255 mm - simulations have been carried out under quasi-static conditions.

Thanks to the axial-symmetric geometry of the membrane, we have first meshed a radial section of the diaphragm and successively the 3D mesh has been obtained by revolving the 2D mesh around the membrane axis of symmetry [2,3].

BOUNDARY CONDITIONS FOR F.E.M. SIMULATION

In order to simulate the behaviour of the membrane during the pumping action by means of the f.e.m., all the actions due to those parts of the pump that interact directly or indirectly with the membrane have been transformed into analytical conditions on the nodes of the 2D mesh [4].

Figure 4 shows a synthetic scheme of the boundary conditions that have permitted us to simulate the working conditions of the pump. Each physical boundary condition can be transformed therefore into an analytical expression as follows:

1. In order to respect the axial-symmetry hypothesis for the membrane, it has been necessary that the node set on the symmetry axis of the membrane cannot move in a radial direction, i.e. the nodes cannot change their abscissa:

$$x_i = 0 \tag{1}$$

2. Condition of non-penetration between the membrane and the oil refill valve ❶.

$$y_i < h \tag{2}$$

3. Condition of non-penetration between the membrane and the cap in the pumping head ❹.

$$y_i > \mathrm{Y}_4(x_i) \quad \forall \mathrm{P}_{i1} \tag{3}$$

4. Condition of contact and adherence for all nodes in contact with the ledge ring ❸.

$$y_i = 0 \tag{4}$$

5. Limitation of sliding for the nodes on the border of the membrane in order to avoid the penetration of element ❷ into the clamping zone during the assembling operation.

$$x_i < d \tag{5}$$

6. During the assembling operation operation, the clamping caused by elements ❷ and ❹ leads to squashing of the membrane border, so that this part is fully deformed (see figure 5).
   The assembling operation has to be simulated by means of an iterative cycle divided into *n* steps. Let *s* be the amount of the displacement due to the clamping. At the first step, the element ❷ and the membrane are tangent and ❷ has an ordinate equal to δ^*. At a general j^{th} step the ordinate becomes:

$$\delta_j = \delta^* - j \cdot s / n \quad (j = 0,..., n) \tag{6}$$

   At the end of the cycle, the ordinate of element ❷ is equal to $\delta^* - s$. At each j^{th} step, for all the P_{ih} nodes of the membrane that satisfy the condition:

$$y_i^{(k-1)} > \mathrm{Y}_2\left(x_i^{(k-1)}, \delta_k\right) : \delta_k = \delta^* - k\, s/n, \forall k = 1, 2, \ldots, j \tag{7}$$

the following shift is imposed:

$$\sum_{k=1}^{j} \min\left(0, \left(\mathrm{Y}_2\left(x_i^{(k-1)}, \delta_j\right) - y_i^{(k-1)}\right)\right) \tag{8}$$

7. Limitation of sliding for all those nodes that are in contact on segments CD and BA of element ❷ (see figure 6):

$$x_i \le \mathrm{X}_2^{\mathrm{AB}}\left(y_i^{(n+1)}, \delta\right) \ \forall \mathrm{P}_{i\mathrm{h}} \in \mathrm{AB} \tag{9}$$

$$x_i \ge \mathrm{X}_2^{\mathrm{CD}}\left(y_i^{(n+1)}, \delta\right) \ \forall \mathrm{P}_{i\mathrm{h}} \in \mathrm{CD} \tag{10}$$

   These conditions prevent penetration between the membrane and element ❷ during loading. This is thanks to the displacement towards *x* direction of the nodes that belong to the zone involved in the clamping operation.

8. Boundary condition imposed on the membrane deformation: during the membrane deformation, the volume of the oil held in chamber ② of figure 2 must be constant, as a consequence of the displacement of the plunger. The analytical expression of this condition can be obtained by considering that the value depends on the profile of the upper part of the membrane. Let us take Γ_0 as the profile of the non-deformed membrane and Γ_1 as the profile corresponding to a general deformed shape.

   Thanks to the axial-symmetric geometry of the membrane it is easy to express the volume of chamber ② as (see figure 7):

$$V_{\Gamma_0} = K_0 - 2\pi \int_0^{r_{\max}} \rho \Gamma_0(\rho) d\rho \tag{11}$$

   when the membrane is not deformed, while as a consequence of a deformation it becomes:

$$V_{\Gamma_1} = K_0 - 2\pi \int_0^{r_{\max}} \rho \Gamma_1(\rho) d\rho \tag{12}$$

   Since the volume of the oil must be constant, $V_{\Gamma_1} = V_{\Gamma_0}$, therefore the right hand sides of eqs. (11) and (12) have to be equal:

$$K_0 - 2\pi \int_0^{r_{max}} \rho \Gamma_1(\rho) d\rho = K_0 - 2\pi \int_0^{r_{max}} \rho \Gamma_0(\rho) d\rho \Rightarrow \int_0^{r_{max}} \rho \Gamma_1(\rho) d\rho = \int_0^{r_{max}} \rho \Gamma_0(\rho) d\rho \quad (13)$$

By considering the co-ordinates of the nodes that belong to the upper profile of the membrane at the n+1 step of the clamping simulation, we can write:

$$2\pi \int_0^{r_{max}} \rho \Gamma_0(\rho) d\rho \approx 2\pi \sum_{i=2}^{N} x_i^{(n+1)} y_i^{(n+1)} \left(x_i^{(n+1)} - x_{i-1}^{(n+1)} \right) = k \quad (14)$$

Function $\Gamma_1(x)$ is unknown. Nevertheless this problem can be overcome by considering a generic node that belongs to the upper profile of the membrane with co-ordinates $\left(x_i^{(n+1)}, y_i^{(n+1)} \right)$ and by supposing that, during the membrane deformation due to the working pressure, it changes only its ordinate from $y_i^{(n+1)}$ to $y_i^{(*)}$. This hypothesis can be justified by taking into account the axial-symmetry of the membrane and the small amount of horizontal displacements. With this new hypothesis it results that:

$$2\pi \int_0^{r_{max}} \rho \Gamma_1(\rho) d\rho \approx 2\pi \sum_{i=2}^{N} x_i^{(n+1)} y_i^{(*)} \left(x_i^{(n+1)} - x_{i-1}^{(n+1)} \right) \quad (15)$$

Consequently, with $\gamma_i = y_i^{(*)}$ and $M = N - 1$, the condition expressed by eq. (13) can be rewritten as the following linear boundary condition:

$$\sum_{i=1}^{M} a_i \gamma_i = k \quad (16)$$

The most interesting aspect of this approach is that we can directly simulate the movement of plunger ① of figure 2 and therefore its effect on the membrane deformation. This is possible by imposing a constant value for the volume of oil moved during a plunger stroke, simply by changing the eq. (16) as follows:

$$\sum_{i=1}^{M} a_i \gamma_i = k - \mathrm{V}_c(c) \quad (17)$$

9. The pressure of the fluid in the pumping head can be introduced by declaring which nodes are involved in its action, i.e. all those with a side towards the process fluid.

ANALYSIS OF THE SIMULATION RESULTS

The behaviour of the standard design membrane (outside diameter 255 mm) has been studied when the fluid is pumped into the outlet circuit. This occurs when the pressure in the pumping head ④ of figure 2 is equal to the pressure in the outlet circuit. This pressure can range from 5 to 35 MPa, depending on varying working conditions

Before showing the results of the simulation, it is worthwhile making some comments about the simulation procedure.

The process by which the membrane is closed in the clamping seat during the operation of the pump preliminary assembly is schematically shown in figure 8. The membrane conforms to the shape of the clamping support.

The compression due to the metallic support (see ❷ in figure 4) causes the squashing and the stretching of the rubber so that it conforms to the prismatic shape of the support and ensures a good sealing. The great difference in elastic modulus between rubber and *Teflon* causes a high stress concentration in rubber and *Teflon* interfaces. The simulation results for the value of shearing stress is shown in figure 9.

It has been verified by the simulations that, during the pumping action, the membrane bends and slips periodically on the edge of the support ring (see ❸ in figure 4). The cracks observed on the *Teflon* layer may be due to this action.

Some simulations on samples with different geometries have made it evident that stress and stretch increase when the thickness and the length of the rubber layer increase.

The membranes constructed according to the current design are thin and are very thick in the middle. If a 30 MPa pressure is applied to the diaphragm, removing the oil refill boundary (see ② in figure 4), the membrane behaviour is shown in figure 10.

The membrane, whose stretch is due to pressure action, must satisfy the boundary condition on the volume preservation (see ⑧ in figure 4). So the rise of the profile in the middle part must be compensated for the lowering of the area enclosed by the two concentric peripheral circles.

As follows from the results of the simulation, we observe a high stress concentration at the membrane points where the thickness of the rubber is highest.

By reintroducing the boundary condition of the refill valve ② in figure 4, we have observed that Von Mises' index increases more than 20% near the symmetry axis. As a consequence of the presence of the *refill* valve, the membrane cannot rise in its central part and so the rubber is forced to slide. This fact causes a higher deformation of the *Teflon* layer and the stress increases.

The lower displacements in the peripheral zone decrease the bending of the membrane in the clamping zone and the stresses near ring ❸ (see figure 4) are reduced.

The particular design of the *Teflon* layer (see figure 3), has negative stiffness effects on the diaphragm that must be in addition to those due to the high Young's modulus typical of *Teflon*. Some lower profiles of the *Teflon* layer are shown during the pumping action with a 35 MPa working pressure in figure 11.

Observations on the membrane movement

The behaviour of the central part of the membrane is shown as a function of the plunger stroke in figure 11. The more the stroke increases the wider the concavity becomes and the more the inflexion point F moves towards the centre of the membrane. The central zone of the diaphragm follows the deformation of the other zones only for the highest values of the stroke. The consequence of this fact is that, in normal working conditions, only one part of the membrane is really active and determines the pumping action.

This kind of behaviour occurs especially at high pressure. The plunger stroke, at which the membrane comes off valve ❶, is not constant, but increases with pressure. Indeed at the higher operating pressures, the membrane becomes more and more deformed and tends to get the shape shown in figure 10.

The stresses resulting from simulations can be classified in three categories: shearing stresses that are concentrated at the joint between rubber and *Teflon*, which were already made evident by the analysis of clamping operation. Stresses due to bending of the membrane close to the steel ring edge (see ❸ in figure 4) and those located in the central zone of the membrane, due mainly to the different stretch of rubber and *Teflon.* Figure 3 shows three zones (1,2,3) in which the highest stress values have occurred The following comments are common to all simulated conditions.

In zone 1 the stresses increase with the volume of oil moved by the plunger The variations are usually small and occur within a range of 10 MPa. On the other hand, it is very interesting that stresses in the clamping zone do not seem to be influenced by the increasing pressure, as the elements of the seal limit the deformation in this area, by isolating it from the other zones of the membrane.

In zone 2 both the plunger stroke and the pressure increase stress.

In zone 3, the highest stress occurs with the null plunger stroke. In this situation the membrane is compressed towards the oil refill valve ❶ in fig. 4 and transfers the deformation completely onto the *Teflon* layer.

DESIGN IMPROVEMENT OF THE MEMBRANE

Since the problems of the current design have been characterised, an improved design has been realised, by using the following criteria.

1. Clamping: the upper shape of the membrane in this zone has been left unchanged so that design changes in other parts involved in the clamping operation are not necessary (we refer in particular to clamping part ❷ and the knurled ring ❸ in figure 4). This permits us to utilise the membrane with this new shape as a substitute for the old ones.

   The layer made of *Teflon* has been deigned with a special corrugation in order to avoid wear on *Teflon* as a result of its rubbing on the support ring ❸. This corrugation increases the stiffness of the *Teflon*, so that it cannot rub on the support ring edge for each value of designed outlet pressure and plunger stroke.
2. Thickness: the thickness of the *Teflon* layer, which was uniform in the original design, has been left unchanged, while the thickness of the rubber - which was extremely variable - has been made as uniform as possible.
3. Shape: several simulations with different shapes of the membrane have shown that a great reduction of the sweep in the profile of the membrane permits us to obtain a “flatter” membrane with:
   a) a deformed shape similar to a sphere at both low and high pressure, so that the membrane adapts itself better to the pumping head;
   b) a uniform distribution of stress in the *Teflon* layer with low pressure load;
   c) stress values, also at a higher outlet pressure, which are lower than in the original design.
4. Corrugations: some low amplitude corrugations on the *Teflon* layer have been introduced in order to increase the elasticity at the most critical zones of the membrane for example: the central zone, which is especially stressed at high pressure, and that is close to the support ring in which there is the highest stress at the maximum plunger stroke.

The membrane designed following the previous criteria is shown in figure 12.

The behaviour of new membrane has been simulated in the same working conditions as that of the original design. Its behaviour is not very different at low pressure, while there is a remarkable improvement at high operating pressure.

Figure 13 shows the comparison between the clamping zone of the two membranes subject to 30 MPa pressure and maximum plunger stroke. These correspond to the operating conditions for which bend effect is the maximum. It is evident from the comparison of figures (a) and (b) that in the newly designed membrane the *Teflon* does not touch the edge A of the ring; furthermore the shearing stress close to A is lower.

Thanks to the moderate lengthening of new designed membrane, the deformation without boundary condition ② (the oil refill valve) shown in figure 14 is not very different from the deformation with the boundary condition even at a pressure of 30 MPa. In the light of this consideration, we can observe that there is little interference between the improved design membrane and valve ❶ in figure 4. Therefore in this case the stresses in the central part of the diaphragm are reduced.

A confirmation of this fact is that the maximum value of the stress index for the improved design membrane shows only a 2% change between the condition with and without boundary ②, while the current design membrane shows a 20% change.

Figure 15 shows the lower profile of the improved membrane and its similarity to an arc of circumference when the plunger stroke changes. Moreover it is evident that the whole profile contributes to the pumping action for low flow rates as well, so that deformations and stresses are distributed.

Moreover, stresses are decreased in all the zones shown in figure 3. Since the design improvement of the membrane has not involved the border part of the profile, stresses in zone 1 are approximately equal to those of the current membrane. Consequently previously expressed observations remain valid.

In zone 2, as already observed, there is a great decrease of the stress index even for high operating pressures.

In zone 3 the maximum stress index is closely related to the working pressure, while it is minimally dependent on the plunger stroke changing. It remains lower than current membrane shape, under the same working conditions. This is due to the shorter length of the membrane subject to the operating pressure (due to the inferior rubber thickness used and the shorter length of the profile) and to the inferior resistance to the tensile stress thanks to the corrugated shape of the *Teflon* layer.

CONCLUSIONS

An f.e.m. has permitted us to simulate the behaviour of a membrane incorporated in a metering pump. The aims of the simulations were the study of deformation, stress, behaviour and anomalous stress concentration under both normal and heavy duty working conditions with high pressure loads.

Analytical models of the boundary conditions relative to parts of the pump that are in contact with the membrane have been created; other models have been created to simulate typical characteristics of the pump.

The simulations have permitted us to point out the following problems for the membrane of current design:

- high stress concentration near the support ring in the clamping zone;
- non functional deformation at both low and high pressure;
- relevant stress increase in the central zone of the membrane when the working pressure increases.

Those observations have permitted us to improve the design of the membrane, with the following results:

- elimination of rubbing between the *Teflon* layer and the support ring in the clamping zone;
- the deformations of the new membrane are smaller than the current membrane ones, for every operating pressure and flow rate;
- lower stress concentration in the central zone of the membrane;
- the behaviour of the membrane is less sensitive to the variations in working conditions.

ACKNOWLEDGMENTS

The authors wish to thank O.M.G. (Officine Meccaniche Gallaratesi) for technical and financial help. They also wish to thank Dr. Emanuele Osto and Dr. Luca Venegoni for their helpful and irreplaceable collaboration. A special thanks goes to Dr. Fabio Carli for his useful suggestions for the mesh modelling and for the f.e. analysis tools supplied.

REFERENCES

1. Fritsch H, Jarosch J, Horn W. Klassifizierung von Dichtungen an Pumpen unter besonderer Berucksichtigung von Membranpumpen. Pumpen + Kompressoren; November 1995: 93-102.
2. Huebner KH, Thornton EA. The finite element method for engineers. J. Wiley; 1995.

3. Zienkiewicz OC, Taylor RL. The finite element method. McGraw Hill; 1989-91.

4. Samtech. Bacon references. 1998; vol M2a, M2b, M2c.

NOMENCLATURE

P_{ih}	i^{th} node that belongs to the upper profile of the section of the membrane.	$\Gamma_1(x)$	analytical expression of the upper profile of the section of the membrane exposed to the working pressure (c=0).
P_{il}	i^{th} node that belongs to the lower profile of the section of the membrane.	$\Gamma_2(x)$	analytical expression of the upper profile of the section of the membrane exposed to the working pressure and to the plunger stroke c ($c \neq 0$).
$x_i^{(j)}$, $y_i^{(j)}$	abscissa and ordinate of point P_{ih} at the j^{th} step of the assembling operation of the membrane.	N	number of the nodes P_{ih} that are not in contact with element ❷ after the assembling operation (see fig. 4).
$y_{i,c}^{(*)}$	ordinate of point P_{ih} when the membrane is exposed to the working pressure and c plunger stroke.	V_{Γ_0}	volume of chamber ② (see fig. 2) when working conditions determines the profile $\Gamma_0(x)$ for the membrane.
$Y_2(x,\delta)$	analytical expression of lower profile of element ❷ (see fig. 4).	V_{Γ_1}	volume of chamber ② (see fig. 2) when working conditions determines the profile $\Gamma_1(x)$ for the membrane.
$X_2(y,\delta)$	inverse function of $Y_2(x,\delta)$.	V_{Γ_2}	volume of chamber ② (see fig. 2) when working conditions determines the profile $\Gamma_2(x)$ for the membrane.
$Y_4(x)$	analytical expression of profile of element ❹ (see fig. 4).	r_{max}	abscissa at witch begins contact between rubber and steel ledge in the clamping zone after assembling operation.
c	plunger ① stroke (see fig. 2).	K_0	constant volume independent of the membrane deformation.
$\Gamma_0(x)$	analytical expression of the upper profile of the section of the membrane after the assembling operation.	$V_c(c) = \left(\frac{\phi}{2}\right)^2 \pi\, c$	volume of oil moved by a plunger that has ϕ diameter and c stroke (see ① in fig. 2).

FIGURE CAPTIONS

Figure 1 – Operating schemes of Metering plunger and plunger-diaphragm pump.

Figure 2 – Main parts of the pump.

Figure 3 – Radial half section of the diaphragm.

Figure 4 – Scheme of the parts of the pump and boundary conditions on nodes of the mesh.

Figure 5 – Progressive deformation of the membrane borders during initial assembling operation.

Figure 6 – In order to avoid penetration of the membrane by element ❷, boundary conditions have been applied to the nodes that belong to segments AB and CD.

Figure 7 – Graphic representation of analytical expressions of the profile of the membrane when boundary conditions change.

Figure 8 – Deformation scheme of the membrane border during the operation of the pump preliminary assembly.

Figure 9 – Distribution of shearing stress τ_{xy} in rubber / *Teflon* interface.

Figure 10 – Von Mises' index and membrane deformation when the operating pressure is equal to 30 MPa, without the boundary condition of the refill valve ❶ (figure 4).

Figure 11 – Lower profile of the current design membrane for different plunger strokes and 35 MPa operating pressure.

Figure 12 – Outline of the section of new improved membrane.

Figure 13 – Comparison between the components of shearing stress τ_{xy} that shows stress states of the two membranes subject to 30 MPa pressure and maximum plunger stroke: (a) clamping zone in the current design membrane; (b) clamping zone in the improved design membrane.

Figure 14 – Stress state (Von Mises' index) and deformation for new design membrane subjected to 30 MPa without the boundary condition of the refill valve ❶ in figure 4.

Figure 15 – Lower profile of the improved membrane for different for plunger stroke and 35 MPa operating pressure.

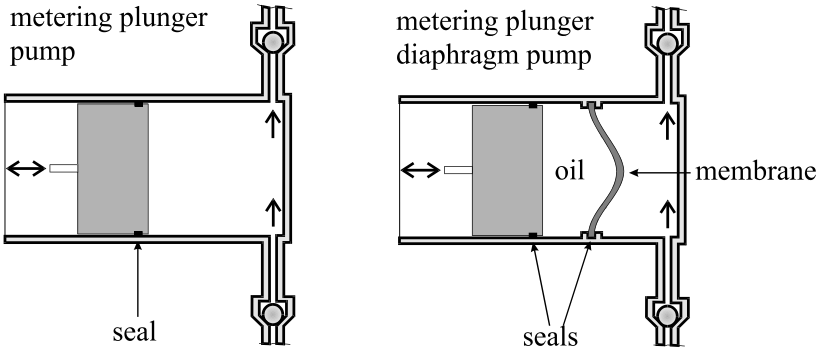

Figure 1 – Operating schemes of Metering plunger and plunger-diaphragm pump.

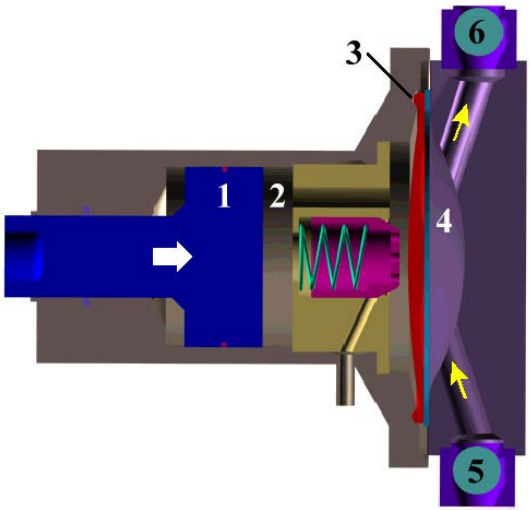

Figure 2 – Main parts of the pump.

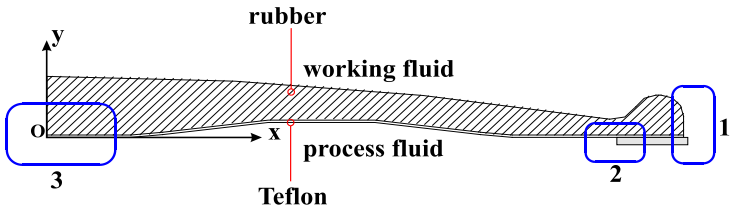

Figure 3 – Radial half section of the diaphragm.

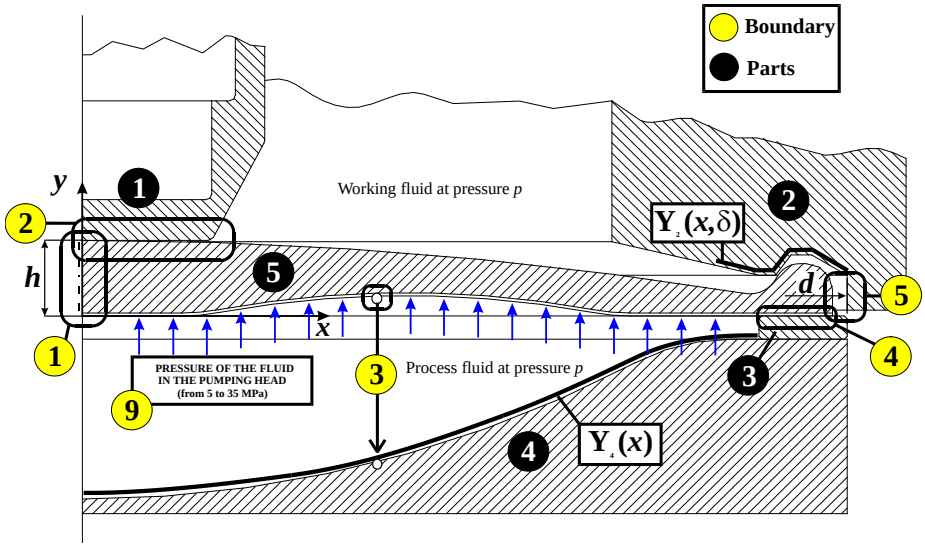

Figure 4 – Scheme of the parts of the pump and boundary conditions on nodes of the mesh.

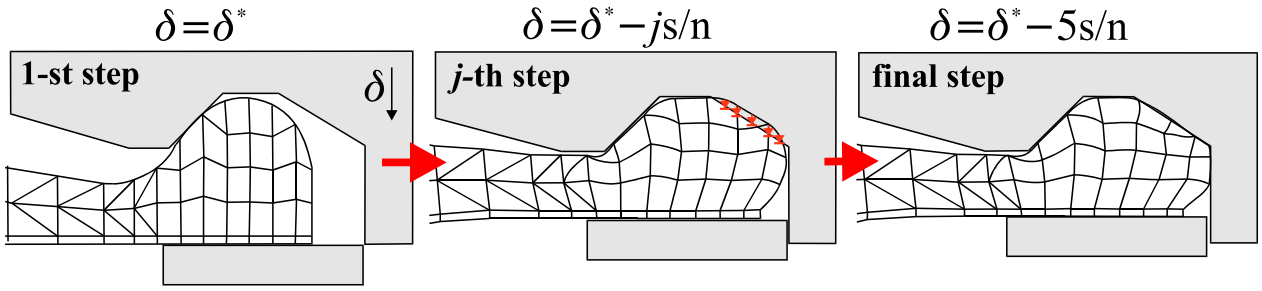

Figure 5 – Progressive deformation of the membrane borders during initial assembling operation.

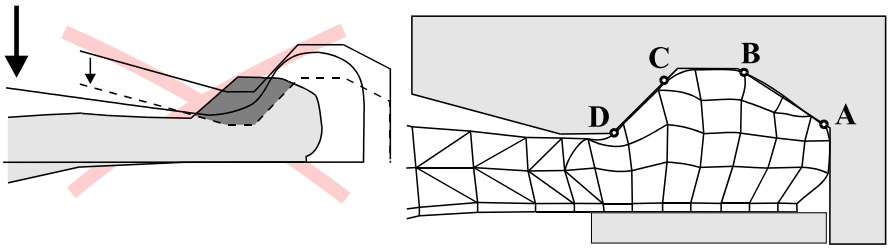

Figure 6 – In order to avoid penetration of the membrane by element ❷, boundary conditions have been applied to the nodes that belong to segments AB and CD.

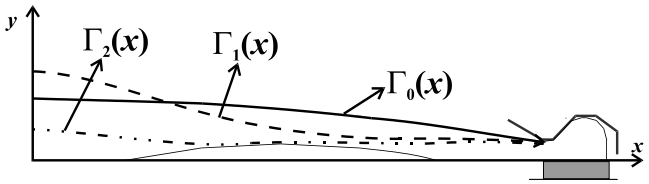

Figure 7 – Graphic representation of analytical expressions of the profile of the membrane when boundary conditions change.

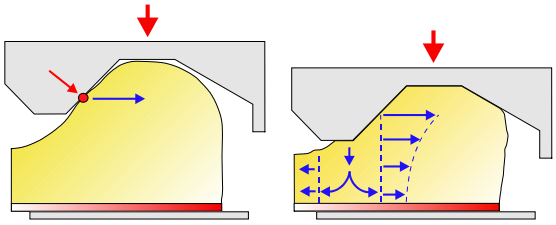

Figure 8 – Deformation scheme of the membrane border during the operation of the pump preliminary assembly.

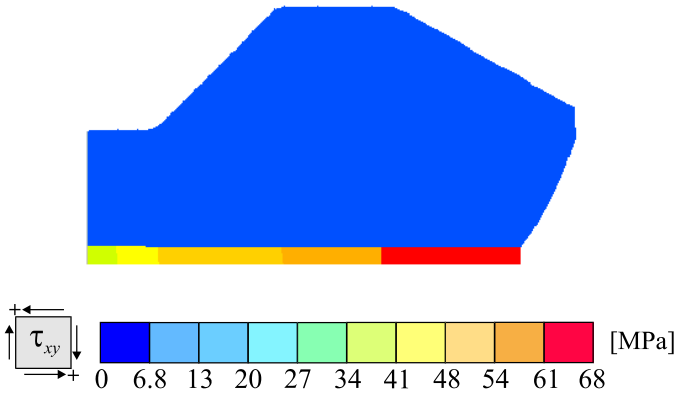

Figure 9 – Distribution of shearing stress τ_{xy} in rubber / *Teflon* interface.

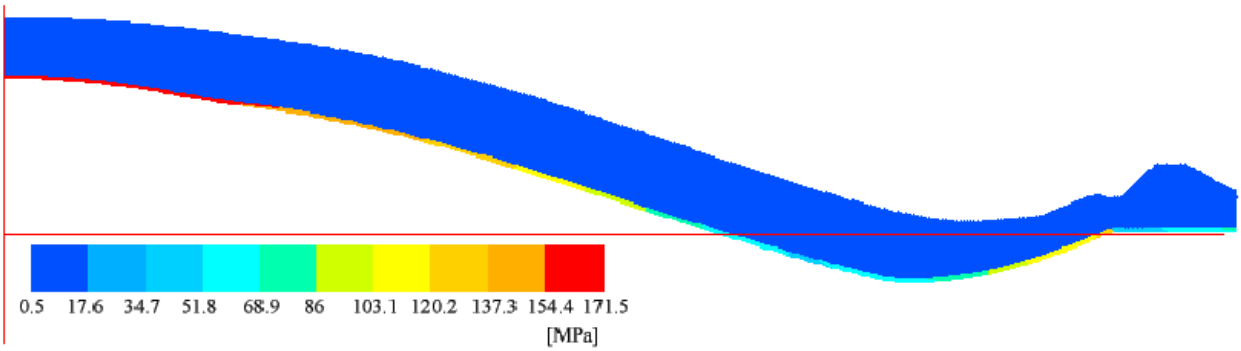

Figure 10 – Von Mises' index and membrane deformation when the operating pressure is equal to 30 MPa, without the boundary condition of the refill valve ❶ (figure 4).

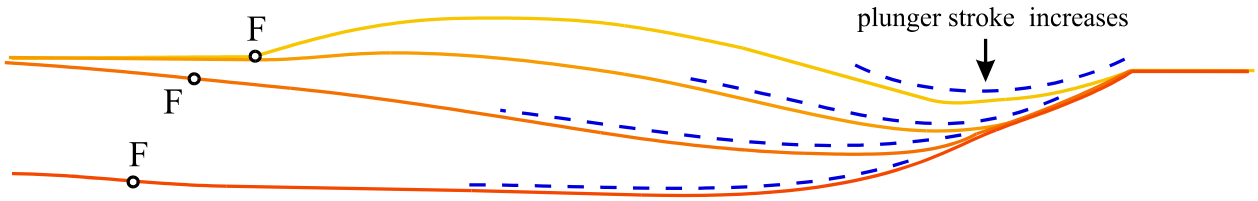

Figure 11 – Lower profile of the current design membrane for different plunger strokes and 35 MPa operating pressure.

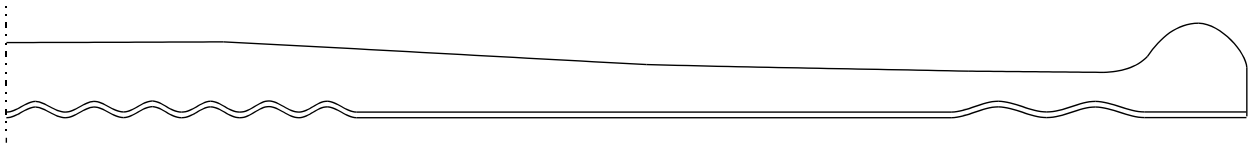

Figure 12 – Outline of the section of new improved membrane.

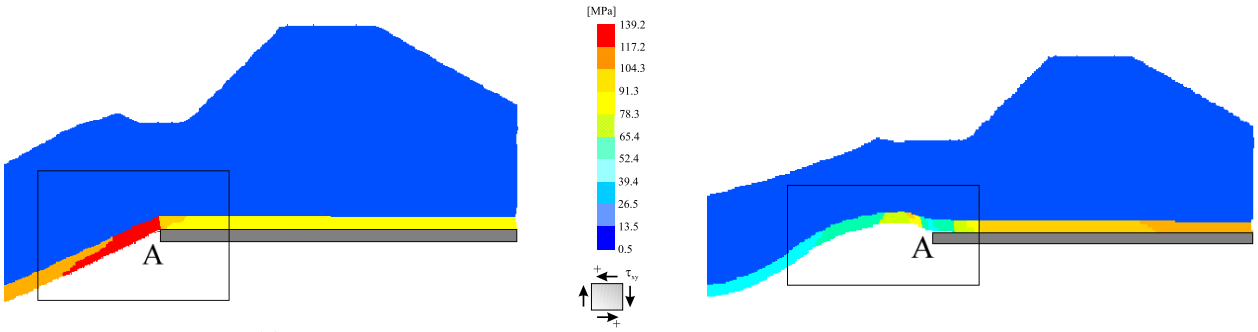

Figure 13 – Comparison between the components of shearing stress τ_{xy} that shows stress states of the two membranes subject to 30 MPa pressure and maximum plunger stroke: (a) clamping zone in the current design membrane; (b) clamping zone in the improved design membrane.

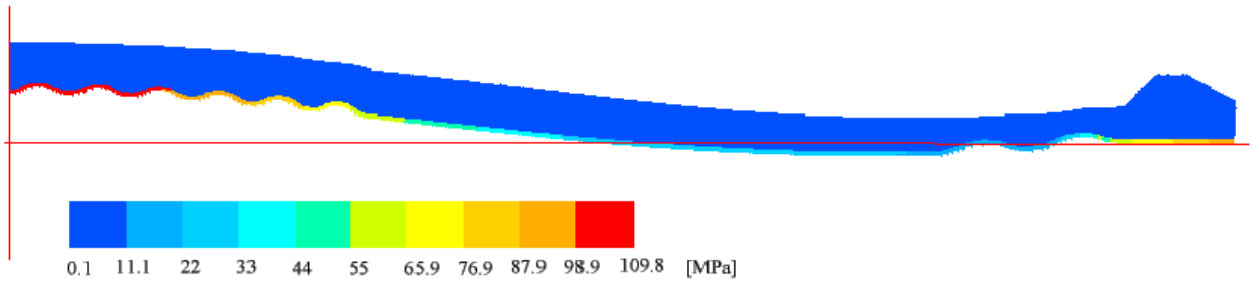

Figure 14 – Stress state (Von Mises' index) and deformation for new design membrane subjected to 30 MPa without the boundary condition of the refill valve ❶ in figure 4.

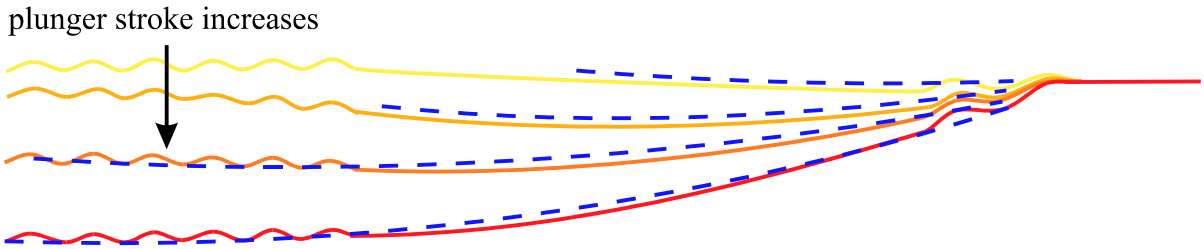

Figure 15 – Lower profile of the improved membrane for different for plunger stroke and 35 MPa operating pressure.